Orthogonally functionalizable polyacetals: A versatile platform for the design of acid sensitive amphiphilic copolymers

Adrian Moreno, Gerard Lligadas, Juan Carlos Ronda, Marina Galià and Virginia Cádiz*

Universitat Rovira i Virgili, Departament de Química Analítica i Química Orgànica, Laboratory of Sustainable Polymers, Marcel.lí Domingo 1, 43007 Tarragona, Spain

ABSTRACT

To expand the range of hydrolytically degradable functional polymers, copolyacetals of various compositions were synthesized and fully characterized, and their self-assembly into nanoparticles was studied. First, functionalized copolyacetals were obtained by polyaddition of alkyne- and activated ester-functionalized diols with 1,4-butanediol divinyl ether (DVE). Second, the copolymers were functionalized by using two orthogonal chemical reactions, the thiol-yne click reaction and transesterification/amidation. Amphiphilic copolymers of varing compositions, i.e. different hydrophilic/hydrophobic balance, were obtained and self-assembled in water to afford well-defined nanostructures. The size of the micelles and the critical micelle concentration were correlated to the chemical nature and to the modification degree of the copolymers. The micelles displayed high drug loading capacity and encapsulation efficiency and could be disassembled in mildly acidic media showing a pH-dependent drug release behavior. Subsequent orthogonal modification to introduce folic acid moieties allowed the preparation of site-specific drug delivery systems, showing the versatility of this approach.

Introduction

In recent years, a renewed interest in degradable polymers for biomedical and engineering applications has led to intensive research.[1-3] Polymers that degrade rapidly show tremendous opportunities for the development of new materials that break down in natural environments as well as for drug delivery applications. Due to their acid-sensitive nature, acetal groups are excellent candidates for facilitating degradation because pH gradients are ubiquitous in the environment and within biological systems.[4] The structural variations of the acetal moiety affect its sensitivity, thus allowing the fine-tuning of degradation.[5] Their incorporation in the main chain or as pendant group of a non-degradable backbone and their use in a variety of areas including controlled release, nucleic acid delivery, degradable polymers, lithography or reshapeable crosslinked materials have been reported.[6-12] Routes to main-chain acetal-containing polymers can be delivered by two general approaches, the polymerization by formation of the acetal bond and the polymerization of acetal containing monomers.[4] The first one includes the reaction of polyols with carbonyl compounds, the reaction of diols with vinylethers and the transacetalization or acetal exchange reactions.[13,14] The second group comprises the polymerization by different techniques which do not involve the acetal group, including step growth, metathesis or cationic ring opening polymerizations.[15-18]

However, despite such widespread use, polyacetals are a class of polymers that was not extensively investigated compared to other polycondensation polymers. In particular, the development of functional polyacetals with diverse properties, which can be accessed from monomers commercially available on large scale, remains unexplored. Polyacetals bearing reactive functional groups provide the opportunity of postpolymerization modification, thus offering control over material properties and broadening the range of potential applications.

Herein, we report a series of functional polyacetals and copolyacetals obtained from derivatives of 2,2-bis(hydroxymethyl)propionic acid (bis-MPA), which is a well-known building block for polyurethane and polycarbonate formulations and widely commercially available at low cost. Bis-MPA can be easily derivatized through the carboxylic acid group to obtain monomers which bear different functional groups.[19-21] In this work, chemically orthogonal alkyne and active ester containing monomers (Scheme 1) have been used. Among active esters, hexafluoroisopropyl esters were chosen as they have been shown to be reactive under transesterification and aminolysis reactions, providing functionalization strategies for polymer modification.[22] Hence, a single-type of polyacetal can selectively react by sequential orthogonal polymer reactions such as activated amidation or transesterification[23] and thiol-yne click reactions[24] to give various copolymers bearing different functionalities and showing distinct properties. To demonstrate the synthetic versatility of this approach, we introduced the alkyne and activated ester functionalities onto polyacetals by acid catalyzed stepwise polyaddition of functionalized diols to 1,4-butanediol divinyl ether and investigated both modification reactions using a thiol and an alcohol as model compounds.

Since the hydrolysis of acetal units takes place at biologically relevant pH values, polyacetals have been investigated in the field of biomedical applications as drug delivery systems.[25-29] Their pH responsive character is useful to control the release of encapsulated active ingredients. Nanoparticle drug delivery systems based on acetal bonds have attracted wide attention in cancer therapy as the microenvironment of the tumor is weakly acidic, thus their organization will be destroyed to trigger fast release of the drug.[30-33] In this work, click-type thiol-yne reaction was applied to functionalize a hydrophobic polyacetal precursor carrying alkyne groups into four amphiphilic copolymers of different functionalization degree and uniform polymeric micelles of

different sizes were achieved by dissolving the material in water. To illustrate the potential of the obtained copolyacetals as drug delivery vehicles, we investigated the release of curcumin (CUR, 1,7-bis-4(hydroxyl-3-methoxyphenyl)-1,6-heptadiene-3,5-dione), a hydrophobic polyphenolic compound possessing potent antitumor activity.[34]

Site-specific delivery of polymeric drug carriers can be enhanced by incorporating target moieties or specific ligands that direct the carrier to a specific location by interacting preferentially with particular cell receptors.[35-37] Folic acid (FA) has become a popular molecule for targeting attached drugs to cancer cells as a natural ligand of the folate receptor, which is overexpressed on the surface of several cancers.[38-41] To demonstrate the versatility of the copolyacetal containing alkyne and activated ester functionalities, the sequential modification by thiol-yne and transesterification have been carried out. The activated ester approach has been used to introduce the FA targeting group and the potential of the obtained nanoparticles in the release of CUR was investigated.

Experimental section

Materials

The following chemicals were obtained from Aldrich and used as received: diazabicyclo-[5.4.0]undec-7-ene (DBU, 99%), 2-mercaptoethanol (ME, 98%), *p*-toluenesulfonic acid (*p*-TSA, 97%), pyridinium *p*-toluenesulfonate (PPTS, 99%), 1,4-butanediol divinyl ether (DVE, 98%), 1,1,1,3,3,3-hexafluoro-2-propanol (HFIP, >99%), ethanethiol (97%), propargyl bromide (80% wt in toluene), benzyl alcohol (BnOH, 99.8%), folic acid (FA, 97%), dicyclohexylcarbodiimide (DCC, 97%), *N*-hydroxysuccinimide (NHS, 97%), *N*-(3-dimethylaminopropyl)-*N*'-ethylcarbodiimide hydrochloride (EDC·HCl, 99%), 2,2-(ethylendioxy)bis(ethylamine) (98%),

pyrene (>99%), nile red (NR, 99%), curcumin (CUR, 99%), triethylamine (TEA, 99%), dimethylsulfoxide (DMSO, 98%), 2,2-bis(hydroxymethyl)propionic acid (bis-MPA, 99%), Tween® 80 and 2',4'-dimethylacetophenone (DMPA, 98%). Amberlyst ® 15 hydrogen form and dialysis tube membrane (MWCO > 2000) were obtained from Aldrich. Tetrahydrofurane (THF) and dichloromethane (DCM) were purchased from Scharlab and distilled from sodium and calcium hydride respectively before use. Other solvents were purchased from Scharlab and used as received.

Instrumentation

^{1}H NMR,^{19}F NMR and ^{13}C NMR spectra were recorded on a Varian VNMRS400. The samples were dissolved in $CDCl_3$, and spectra were recorded at room temperature with tetramethylsilane (TMS) as an internal standard. All chemical shifts are quoted on the δ scale in ppm.

Size exclusion chromatography (SEC) analyses were performed with an Agilent 1200 series system equipped with an Agilent 1100 series refractive-index detector. The analyses were performed at 35 ºC on the three column system: 3 μm PLgel MIXED-E, 5 μm PLgel MIXED-D, 20 μm PLgel MIXED-A at a nominal flow rate of 1.0 mL/min and a sample concentration of 0.1% w/w in THF as solvent. The calibration curve for SEC analysis was obtained with polystyrene standards from Polymer Laboratories with molecular weights ranging from 500 to 400.000 g/mol.

Transmission electron microscopy (TEM) was performed using a JEOL JEM-1011 TEM microscope. Before the measurement, a drop of solution was placed on a copper grid, which was

allowed to dry at room temperature and after that, stained with phosphotungstic acid for 1 minute prior to the analysis.

Fluorescence spectra were recorded using a Shimadzu RF-5301PC fluorescence spectrometer at room temperature. The samples were excited at 335 nm and the emission spectra were recorded from 350 to 500 nm.

Dynamic light scattering (DLS) measurements were carried out at room temperature using Zetasizer Nano ZS (Model ZEN3500) from Malvern Instruments equipped with a He-Ne laser.

HPLC Determination of released CUR was performed with an Agilent 1260 infinity series system equipped with an Agilent 1260 series ELSD detector. The analyses were performed at 40 ºC on two column systems: 3.5 μm Agilent eclipse C18 and 2.5 μm Kinetix C18 at nominal flow rate of 1.2 mL/min. The eluent was a mixture of acetonitrile/water and the samples were analyzed following a gradient from 100 acetonitrile to 80 acetonitrile over 20 minutes; the CUR retention time (tr) was 2.5 min. The release experiments were conducted by triplicate. The results presented are the average data with standard deviations.

Monomer synthesis and characterization

Diols **M1**, **M2** and **M3** were obtained and characterized as described in the supplementary information (SI-1, SI-2 and SI-3 and Figures S1-S10).

Polymer synthesis

Polyacetals **PA1, PA2** and **PA3** and copolyacetal **PA2,3** (Scheme 1) were synthesized according to the following general procedure: a flame dried 10 mL round-bottom flask was charged with 2.97 mmol of diol and PPTS (0.05 mmol) under argon flow. After that, 1.5 mL of dry DCM and

DVE (3.09 mmol) were added. The addition of DVE was carried out at 0 ºC and the reaction was held at this temperature for 30 minutes due to its exothermic nature. Then, the temperature was increased to room temperature and the reaction was carried out for 6 hours. At the end of the reaction, 0.4 mL of NaOH 1 M were added and the corresponding polyacetal was precipitated in 200 mL of cold hexane. The obtained polymer was dissolved in 15 mL of DCM, placed in a separation funnel, washed with water and dried over $MgSO_4$. The polymer was isolated by removing the solvent at reduced pressure and drying under vacuum until constant weight.

PA1

M1 (0.48 g, 2.97 mmol), PPTS (37.1 mg, 0.05 mmol) and DVE (0.5 mL, 3.09 mmol) were used. The polymer was obtained as a colorless viscous liquid in a 76% yield. M_n= 16000 g/mol, M_w= 21000 g/mol, Đ= 1.7.

^{1}H NMR [$CDCl_3$, TMS, δ (ppm)] (Figure S11): 4.66 (q, O-C<u>H</u>-O, 2H), 4.15 (q, COOC<u>H$_2$</u>-CH_3, 2H), 3.66 (m, C-C<u>H$_2$</u>-O, 2H), 3.61 (m, O-C<u>H$_2$</u>-CH_2, 2H), 3.51 (m, C-C<u>H$_2$</u>-O, 2H), 3.39 (m, O-C<u>H$_2$</u>-CH_2, 2H), 1.62 (m, O-CH_2-C<u>H$_2$</u>, 4H), 1.27 (d, O-CH-C<u>H$_3$</u>, 6H), 1.25 (t, $COOCH_2$-C<u>H$_3$</u>, 3H), 1.18 (s, C-C<u>H$_3$</u>, 3H).

^{13}C NMR [$CDCl_3$, TMS, δ (ppm)] (Figure S12): 174.6, 100.0, 67.3, 67.2, 65.4, 65.3, 60.5, 47.7, 26.6, 19.6, 18.1, 14.2.

PA2

M2 (0.8 g, 2.97 mmol), PPTS (37.1 mg, 0.05 mmol) and DVE (0.5 mL, 3.09 mmol) were used. The polymer was obtained as a slightly yellow viscous liquid in a 68% yield. M_n= 5600 g/mol, M_w= 13400 g/mol , Đ= 1.9.

^{1}H NMR [$CDCl_3$, TMS, δ (ppm)] (Figure S14): 5.79 (sept, C<u>H</u>-$(CF_3)_2$, 1H), 4.67 (m, O-C<u>H</u>-O, 4H), 3.67 (m, C-C<u>H_2</u>-O, 4H), 3.57 (m, O-C<u>H_2</u>-CH_2, 4H), 3.50 (m, C-C<u>H_2</u>-O, 4H), 3.38 (m, O-C<u>H_2</u>-CH_2, 4H), 1.61 (m, O-CH_2-C<u>H_2</u>, 8H), 1.31 (d, O-CH-C<u>H_3</u>, 6H), 1.24 (s, C-C<u>H_3</u>, 3H).

^{13}C NMR [$CDCl_3$, TMS, δ (ppm)] (Figure S15): 171.4, 121.8, 119.0, 100.0, 67.1, 66.8, 66.7, 66.6, 65.1 (sept, <u>C</u>H-$(CF_3)_2$), 48.4, 26.6, 19.2, 17.3.

^{19}F NMR [$CDCl_3$, $CFCl_3$, δ (ppm)] (Figure S16): -73.3.

PA3

M3 (0.51 g, 2.97 mmol), PPTS (37.1 mg, 0.05 mmol) and DVE (0.5 mL, 3.09 mmol) were used. The polymer was obtained as a yellow pale viscous liquid in a 85% yield. M_n= 17500 g/mol, M_w= 23200 g/mol, Đ= 1.8.

^{1}H NMR [$CDCl_3$, TMS, δ (ppm)] (Figure S18): 4.69 (m, O-C<u>H</u>-O, COO-C<u>H_2</u>-C≡CH, 4H), 3.69 (m, C-C<u>H_2</u>-O, 2H), 3.60 (m, O-C<u>H_2</u>-CH_2, 2H), 3.59 (m, C-C<u>H_2</u>-O, 2H), 3.40 (m, O-C<u>H_2</u>-CH_2, 2H), 2.48 (t, C≡C<u>H</u>, 1H), 1.62 (m, O-CH_2-C<u>H_2</u>, 4H), 1.27 (d, O-CH-C<u>H_3</u>, 6H), 1.24 (s, C-C<u>H_3</u>, 3H).

^{13}C NMR [$CDCl_3$, TMS, δ (ppm)] (Figure S19): 173.8, 100.0, 77.7, 74.9, 67.1, 67.0, 65.5, 65.3, 52.0, 47.9, 26.6, 19.5, 18.0, 17.9.

PA2,3

M2 (0.38 g, 1.49 mmol), **M3** (0.26 g, 1.49 mmol), PPTS (37.1 mg, 0.05 mmol) and DVE (0.5 mL, 3.09 mmol) were used. **PA-2,3** was isolated as a brown viscous liquid in a 84% yield. M_n= 19500 g/mol, M_w=24800 g/mol , Đ= 1.8.

^{1}H NMR [$CDCl_3$, TMS, δ (ppm)] (Figure S21): 5.79 (sept, C<u>H</u>-$(CF_3)_2$, 1H), 4.68 (m, O-C<u>H</u>-O, COO-C<u>H</u>$_2$-C≡CH, 6H), 3.69 (m, C-C<u>H</u>$_2$-O, 4H), 3.59 (m, O-C<u>H</u>$_2$-CH_2, 4H), 3.54 (m, C-C<u>H</u>$_2$-O, 4H), 3.39 (m, O-C<u>H</u>$_2$-CH_2, 4H), 2.47 (t, C≡C<u>H</u>, 1H), 1.61 (m, O-CH_2-C<u>H</u>$_2$, 8H), 1.31-1.21 (m, O-CH-C<u>H</u>$_3$, 12H, C-C<u>H</u>$_3$, 6H).

^{13}C NMR [$CDCl_3$, TMS, δ (ppm)] (Figure S22): 173.8, 171.4, 121.8, 119.0, 100.0, 77.7, 74.8, 67.5, 67.4, 66.7, 66.2, 65.1 (sept, <u>C</u>H-$(CF_3)_2$), 52.0, 48.5, 47.9, 26.6, 19.5, 19.2, 19.1, 17.7.

^{19}F NMR [$CDCl_3$, $CFCl_3$, δ (ppm)] (Figure S23): -73.2.

T*hiol-yne click modification of* ***PA-2,3*** *with ethanethiol. Synthesis of* ***PA2,3-1***

To a 5 mL round-bottom flask, **PA-2,3** (0.3 g, 0.47 mmol of C≡C) was added under argon flow and dissolved with 0.3 mL of anhydrous THF. After that, ethanethiol (0.2 mL, 2.82 mmol) and DMPA (14 mg, 0.05 mmol) were added by a syringe and the mixture was stirred until a homogeneous solution was obtained. The reaction mixture was irradiated using a UV nail-lamp (365 nm x4 lamps x 9 W) at room temperature for 5 minutes. The crude reaction mixture was added to cold hexane, and the obtained oil was treated several times with ethyl acetate. Finally, the polymer was dried under vacuum until constant weight. (90% yield) M_n= 18800 g/mol M_w= 24100 g/mol, Đ= 1.7.

^{1}H NMR [$CDCl_3$, TMS, δ (ppm)] (Figure S25): 5.78 (sept, C<u>H</u>-$(CF_3)_2$, 1H), 4.66 (m, O-C<u>H</u>-O, 4H), 4.39 (dd, COOC<u>H</u>$_2$-CH, 1H), 4.22 (dd, COOC<u>H</u>$_2$-CH, 1H), 3.69 (m, C-C<u>H</u>$_2$-O, 4H), 3.59 (m, O-C<u>H</u>$_2$-CH_2, 4H), 3.54 (m, C-C<u>H</u>$_2$-O, 4H), 3.39 (m, O-C<u>H</u>$_2$-CH_2, 4H), 3.03 (m, COOCH_2-C<u>H</u>, 1H), 2.79 (m, CH-C<u>H</u>$_2$-S-$(CH_2$-$CH_3)_2$, 2H), 2.64-2.57 (m, S-C<u>H</u>$_2$-

CH_3, 4H), 1.60 (m, O-CH_2-C$\underline{H}_2$, 8H), 1.30-1.25 (m, O-CH-C$\underline{H}_3$, 12H, C-C$\underline{H}_3$, 6H, S-CH_2-C$\underline{H}_3$, 6H).

^{13}C NMR [$CDCl_3$, TMS, δ (ppm)] (Figure S26): 174.2, 171.4, 121.7, 119.2, 100.1, 68.2, 67.2, 67.1, 66.8, 66.5, 65.4, 65.1, 48.5, 48.0, 44.2, 34.2, 27.0, 26.6, 25.5, 19.6, 19.2, 18.0, 17. 9, 14.9, 14.7.

^{19}F NMR [$CDCl_3$, $CFCl_3$, δ (ppm)] (Figure S27): -73.2.

*Transesterification modification of **PA2,3-1** with benzyl alcohol. Synthesis of **PA2,3-2***

To a 5 mL round-bottom flask, **PA-2,3-1** (0.5 g, 0.78 mmol of ester) was added under argon flow and dissolved with 0.3 mL of anydrous THF. To this solution, DBU (20 μL, 0.05 mmol) and BnOH (0.12 mL, 1.17 mmol) were added at once and the reaction mixture was stirred at 45 ºC. Aliquots were taken at different reaction times and analyzed by ^{1}H and ^{19}F NMR spectroscopy until complete conversion (5 h). The crude reaction mixture was precipitated in cold hexane and washed several times with ethyl acetate. Finally, the obtained polymer was dried under vacuum until constant weight. (75% yield) M_n= 19200 g/mol , M_w= 23400 g/mol, Đ= 1.8.

Additional post-polymerization modification procedures can be found in the supplementary information (SI4-SI6).

^{1}H NMR [$CDCl_3$, TMS, δ (ppm)] (Figure S29): 7.33 (m, CH_2-$\underline{Bn}$, 5H), 5.13 (s, C$\underline{H}_2$-Bn, 2H), 4.65 (m, O-C$\underline{H}$-O, 4H), 4.39 (dd, COOC$\underline{H}_2$-CH, 1H), 4.22 (dd, COOC$\underline{H}_2$-CH, 1H), 3.68 (m, C-C$\underline{H}_2$-O, 4H), 3.58 (m, O-C$\underline{H}_2$-CH_2, 4H), 3.51 (m, C-C$\underline{H}_2$-O, 4H), 3.38 (m, O-C$\underline{H}_2$-CH_2, 4H), 3.03 (m, $COOCH_2$-C$\underline{H}$, 1H), 2.78 (m, CH-C$\underline{H}_2$-S-(CH_2-CH_3, 2H)$_2$, 2.63-

2.55 (m, S-C$\underline{H}_2$-CH_3, 4H), 1.61 (m, O-CH_2-C$\underline{H}_2$, 8H), 1.30-1.25 (m, O-CH-C$\underline{H}_3$, 12H, C-C$\underline{H}_3$, 6H, S-CH_2-C$\underline{H}_3$, 6H)

^{13}C NMR [$CDCl_3$, TMS, δ (ppm)] (Figure S30): 174.3, 174.0, 134.5, 128.4, 128.0, 127.8, 100.1, 67.5, 67.2, 66.5, 66.1, 65.4, 65.2, 48.0, 46.9, 44.2, 34.2, 27.0, 26.7, 25.5, 19.6, 18.0, 14.9, 14.8.

Empty and dye/drug loaded micelles preparation from functionalized polyacetals

Micelles of the corresponding functionalized polyacetals were prepared in a single-step by solvent exchange methodology. About 50 mg of polyacetal was dissolved in 0.2 mL of acetone and the resulting solution was added dropwise into 10 mL of Milli-Q water under sonication. The solution was sonicated during additional 3 hours to ensure complete evaporation of acetone. The obtained micellar solution was then filtered through a membrane syringe filter (0.22 μm) and the filtrate used to determine the size and morphology of micelles. Drug or dye-loaded micelles were prepared by a similar method described above for blank micelles. Briefly, CUR or NR (2.5 mg) were dissolved together with the polymer (50 mg) in acetone (0.3 mL) and added dropwise into a 10 mL solution of Milli-Q water under sonication. The micellar solution was sonicated for additional 3 hours to evaporate the excess of acetone. In the case of CUR-loaded micelles the whole process was performed in the dark (vials covered by aluminum foil) since CUR is light sensitive. Drug and dye micellar solutions were filtered through a membrane filter (pore size: 220 nm) in order to remove the encapsulated, NR and CUR and finally, the purified micellar solutions were freeze dried.

Determination of critical micellar concentration (CMC)

The CMC was determined using pyrene as fluorescent probe by direct monitoring the emission peaks at 382 nm and 372 nm in the fluorescence spectra. A concentration of the amphiphilic polyacetals ranging from 1.0×10^{-9} to 1.0 mg/ mL was employed and the pyrene concentration was fixed at 6.6×10^{-7} M.

Determination of encapsulation efficiency (EE) and drug loading content (DC)

EE and DC of dye/drug micelles were determined by dissolving a known amount of freeze-dried sample (10 mg, feeding ratio 2.5 mg of CUR/ 50 mg of polymer) in THF and analyzed to determine the quantification of drug/dye concentration. For the determination of NR concentration, the UV absorption for the sample solution was recorded at 541 nm and the amount of NR was determined using a calibration curve method. For CUR loading content determination, samples were excited at a fixed wavelength (λ_{ex} = 420 nm) and emission spectra were recorded using a fluorescence spectrophotometer. Amount of CUR present in each sample were then calculated using a standard calibration curve for CUR. The DC and EE were calculated following eqs 1 and 2, respectively.

DC= (amount of loaded drug)/ (amount of drug-loaded micelles) x100% (1)

EE= (amount of loaded drug)/ (total amount of feeding drug) x100% (2)

Determination of in vitro pH-triggered release of CUR

The release of CUR from amphiphilic polyacetal micelles was investigated at 37 ºC in two different media: phosphate buffer, pH 7.4 and acetate buffer, pH 5.0. The concentration of release media was fixed at 10 mM. The CUR-loaded micelles were divided in two groups (for pH 7.4 and 5.0, each group 5 mL). Then, their pH was adjusted to 5.0 using acetate buffer or maintained at 7.4

using phosphate buffer. After that, 5.0 mL of CUR-loaded micelles dispersions (at a theoretical DC of 5.0%) were transferred to a dialysis tube with a MWCO of 2.0 kDa Materials. The dialysis tube was immersed into a 25 mL of the corresponding buffer containing Tween-80 (0.5 % w/w) at 37 ºC under stirring. After predetermined times, 5.0 mL of release media was taken out for the HPLC analysis and replaced with an equal amount volume of fresh media.

Results and discussion

Acetal polymer synthesis

Diol monomers **M1**, **M2** and **M3** were obtained from bis-MPA following reported procedures (SI 1, 2 and 3, Figures S1-6). [20,42] As a first attempt, the direct conversion of the diol **M1** as a model compound to the corresponding polyacetal by its step growth polymerization with DVE using an acid catalyst was investigated (Scheme 1).

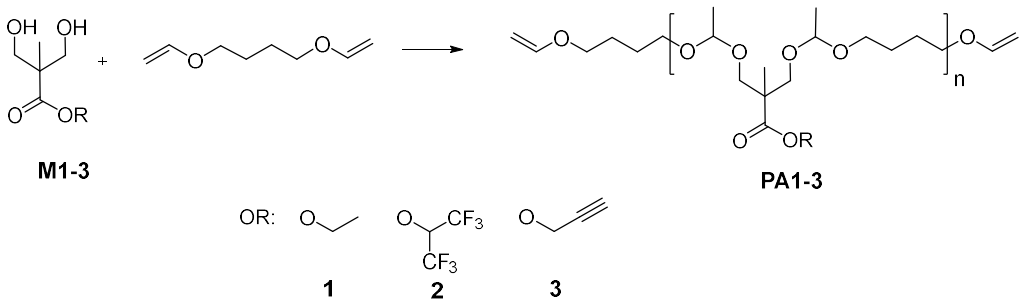

Scheme 1. Synthesis of polyacetals **PA1**, **PA2**, **PA3 and PA2,3**.

The reaction was carried out using PPTS (1.7%) in stoichiometric imbalance diol/DVE 1:1.04 at room temperature. Aliquots of reaction mixture were withdrawn at different time intervals and analyzed by SEC and NMR to determine the extent of the reaction, the degree of polymerization and the molar mass of the resulting polymer. ^{1}H NMR spectroscopy showed the disappearance of signals attributed to the CH_2OH moiety (3.90, 3.73 and 3.01 ppm) of **M1** and to the double bond protons at 4.20 and 6.50 ppm corresponding to DVE. Moreover, the appearance of new signals corresponding to the methyne **5** (4.66 ppm) and methyl signal **6** (1.30 ppm) of the acetal linkage of the polymer can be observed (Figure S11). After 6 h of reaction no significant differences were observed. Hence, this time was fixed as the polymerization time, leading to a polymer with M_n of 16000 g/mol and Đ=1.7 by SEC in a 76% yield. The expected signals for the acetal methyne and metyl can also be seen in the ^{13}C NMR spectrum (Figure S12). No signals due to end groups or indicative of other structures are present either in ^{1}H or in ^{13}C NMR, thus indicating the formation of the expected structure for **PA1**. Polyacetals **PA2** and **PA3** were obtained in a similar way and their spectra are also consistent with the target structures, showing that hexafluoroisopropil and propargyl esters were unaltered under the polymerization conditions (Figures S14-S20). Copolyacetal **PA2,3** was synthesized under the above described conditions using equimolar amounts of **M2** and **M3**. Signals attributable to polyacetal main chain and to both functional groups, the hexafluoroisopropyl and propargyl esters, can be seen in the ^{1}H NMR spectrum (Figure 1a). From the integration of signals **c** and **A** the copolymer composition was found to be 1.1:1.0 in good agreement to the monomers feed.

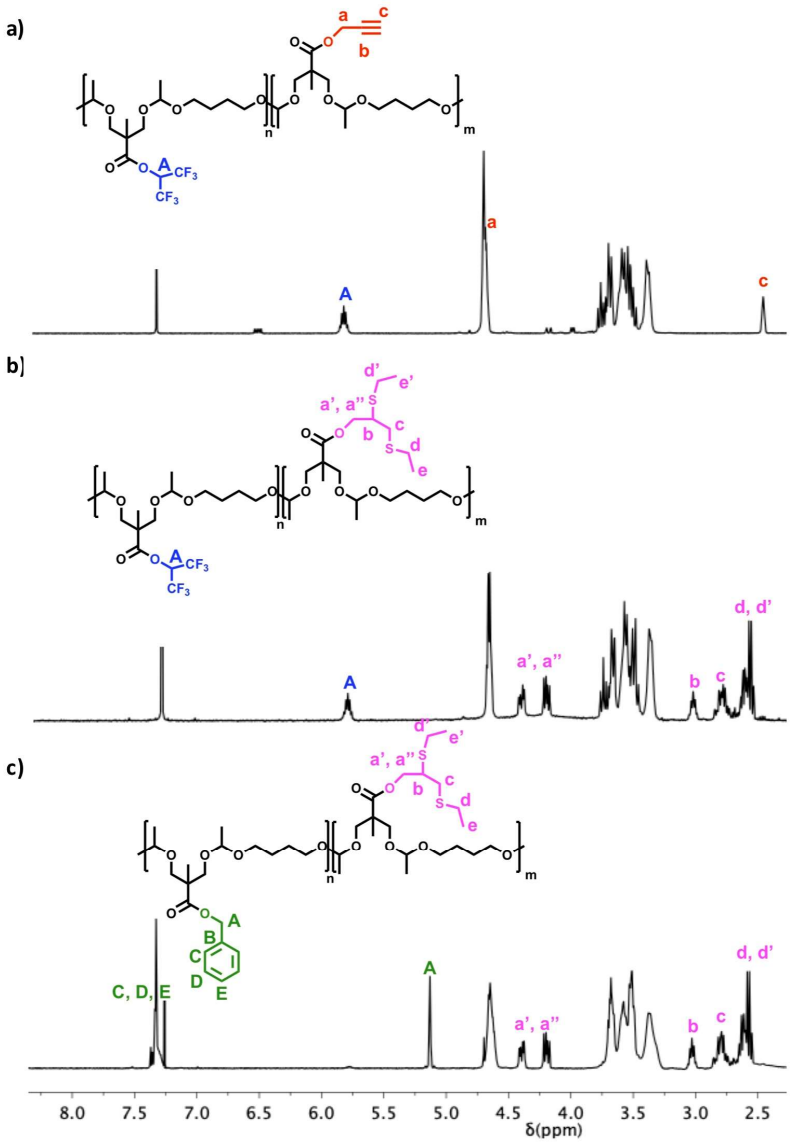

Figure 1. ^{1}H NMR spectrum of a) **PA2,3**, b) **PA2,3-1** and c) **PA2,3-2** (δ (ppm), $CDCl_3$).

The difunctional copolymer was sequentially modified by click type thiol-yne addition and transesterification using model compounds. The first reaction was conducted in the presence of 3 equivalents of ethanethiol under UV irradiation using DMPA as initiator for 5 min. The **PA2,3-1** copolymer was purified and characterized by ^{1}H NMR and SEC. The disappearance of the terminal acetylene protons (2.47 ppm) confirmed the full consumption of the alkyne groups (Figure 1b).

The presence of signals attributable to the diastereotopic methylene protons **a'** and **a''** (4.25 and 4.40 ppm), the methyne proton **b** (3.03 ppm) and methylene protons **c** (2.70 ppm) corresponding to the 1,2-regioselectivity of the thiol-yne addition and the presence of methylene protons **e** and **e'**(1.30 ppm) of the ethane moiety also verified the successful reaction. No signals in the alkene region can be seen, thus indicating the absence of vinylsulfide moieties resulting from the addition of only one thiol molecule across the triple bond. All the signals corresponding to the main chain as well as to the fluorinated ester group remained unaltered, according to the tolerance of the method to the acetal and ester functional groups. The disappearance of end group signals at 6.51, 4.32 and 4.13 ppm can be attributed to the thiol-ene reaction of the vinyl ether, [43] however new signals attributable to the corresponding thioether cannot be distinguish since they are expected to overlap with signals corresponding to thiol-yne addition.

By ^{13}C NMR the disappearance of signals corresponding to the triple bond can be observed (74.6 and 78.9 ppm) (compare Figure S22 and Figure S26). Moreover, the carbon signals corresponding to the addition of ethanethiol can be observed at 44.2, 34.2, 25.5 and 14.9 ppm respectively. SEC analysis showed no significant variations on molecular weight and molecular weight distribution for **PA2,3-1** by comparison to **PA2,3** (Figure 2, compare black with red trace).

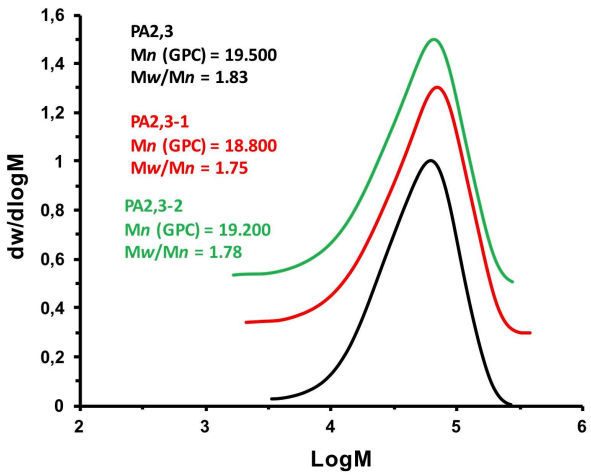

Figure 2. SEC traces of **PA2,3** (black curve), **PA2,3-1** (red curve) and **PA2,3-2** (green curve).

Next, the transesterification of the hexafluoroisopropyl ester was studied using BnOH as a model compound. The reaction was carried out using DBU (5 mol%) and 1.5 equivalents of alcohol at 45 ºC and followed by ^{1}H and ^{19}F NMR spectroscopy. The disappearance of methyne signal of hexafluoroisopropyl moiety at 5.78 ppm and the appearance of methylene and aromatic protons signals (5.13 and 7.33 ppm, respectively) confirmed the complete reaction after 5 h (Figure 1c, Figure S32). Moreover, the ^{19}F NMR spectra showed the disappearance of signal at –73.2 ppm, according to ^{1}H NMR result. Other signals in ^{1}H and ^{13}C NMR spectra were consistent with the expected structure for **PA2,3-2** (Figure S29-S31). Additionally, SEC analysis of the modified polymer showed no significant modification on molecular weight (Figure 2, compare red with green trace). These results are indicative of the controlled nature of the postpolymerization modifications, with no detectable adverse side reactions, that is backbone degradation or side groups undesired modifications, and demonstrates the versatility of this approach to enable the polymer transformation through click processes.

To efficiently serve as a delivery carrier, the polymer must be able to self-assemble into nanostructures that isolate the drug from the hydrophilic environment and deliver it inside the cell. To this aim, the introduction ME through thiol-yne coupling was envisioned to be an approach to self-assembling amphiphilic copolymers. The modification of **PA3** as a model polyacetal (Figure 3a) was carried out under the previously described conditions using 3 equivalents of ME, and a modification degree of 100%, as determined by ^{1}H NMR was obtained, according to the previous results (Figure 3b).

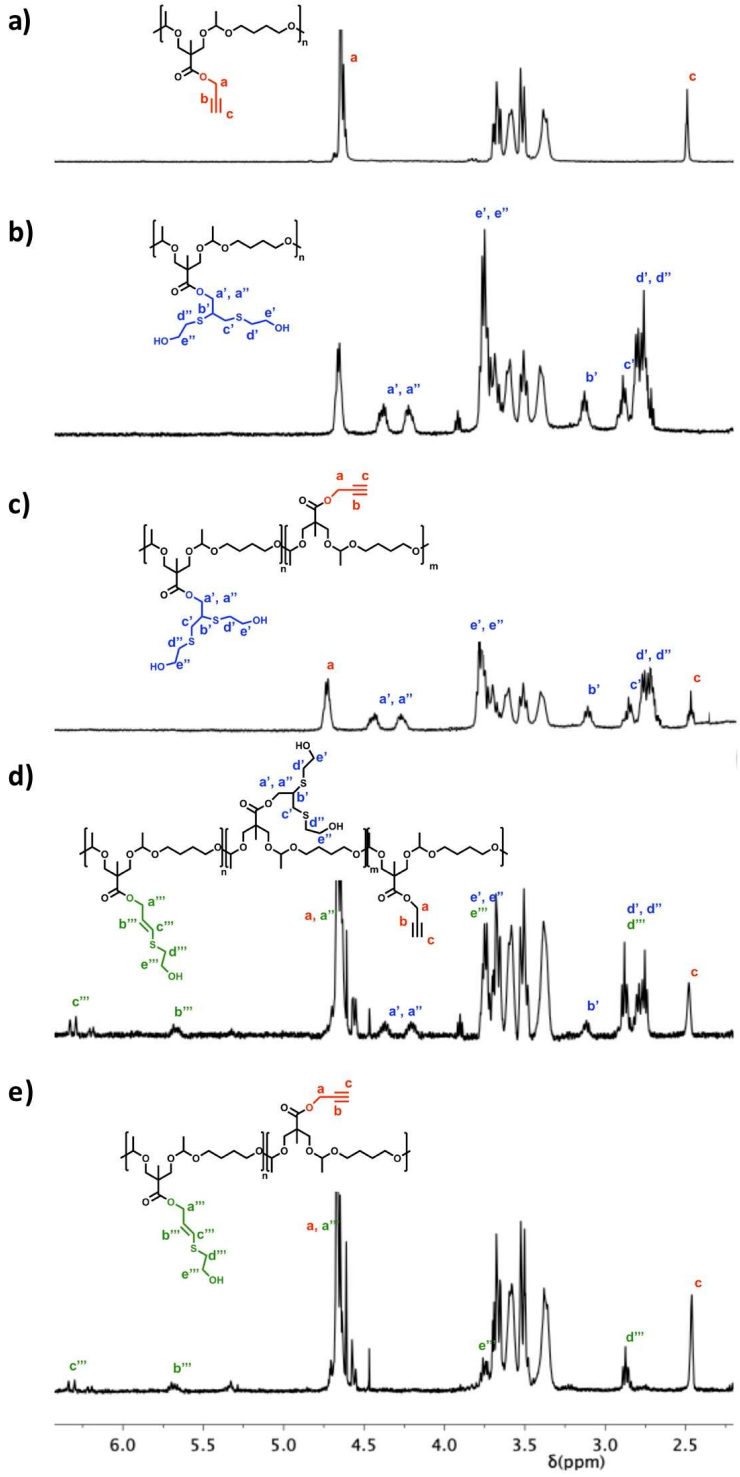

Figure 3. ^{1}H NMR spectrum of a) **PA3**, b) **PA3-100,** c) **PA3-63,** d) **PA3-36** and e) **PA3-14** (δ (ppm), $CDCl_3$).

Lowering the ME amount to 2.1 equivalents, a lower modification degree of 63% was achieved (**PA3-63**). No vinylsulfide units were observed, according to the lower reactivity of the triple bond in front of the double bond (Figure 3c).[44] A further decrease to 1.05 equivalents of ME led to a 36% of modification (**PA3-36**). However, signals attributable to the vinylsulfide could be seen in this case (Figure 3d), thus indicating that both, mono- and di-addition took place (26% and 10%, respectively). Moreover, signals corresponding to the *trans* (6.45 and 5.70 ppm) and cis (6.24 and 5.30 ppm) isomers can be observed. In accordance to these results, the use of 0.65 equivalents of thiol led to a polymer containing a 14% of both, *trans* and *cis* vinylsulfide moieties (**PA3-14**, Figure 3e). In all cases, SEC analysis revealed that the molecular mass of each modified polymer and the Đ did not change significantly (Figure S33).

The functionalization *via* thiol-yne coupling using ME was also applied to **PA2,3** under the previously described conditions for **PA3-100** reaching a modification degree of 100% as confirmed by ^{1}H NMR. In this way, the copolyacetal **PA2,3-3** that contains the hexafluoroisopropyl ester as hydrophobic moiety was obtained (Scheme 2).

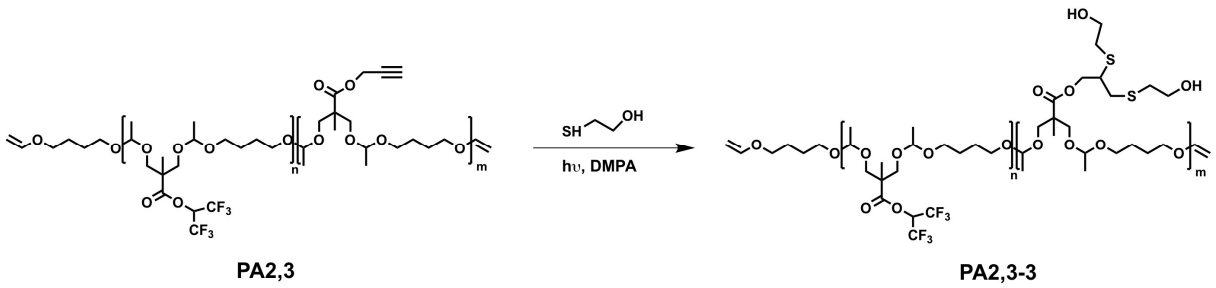

PA2,3 **PA2,3-3**

Scheme 2. Synthesis of **PA2,3-3** through the modification of **PA2,3** *via* thiol-yne reaction with ME.

Nanoparticles formation

The functionalized copolymers were dissolved in acetone and added dropwise to stirring water. Subsequently dynamic light scattering experiments confirmed the formation of stable and monodisperse nanoparticles. DLS measurements for **PA3** derived polymers showed that nanosized particles ranging from 111 to 177 nm were formed, and that the increase of the hydrophilic content resulted in an increase of the particle size as a general trend for **PA3** derivatives (Table 1 and Figure S34). This fact can be reasonably attributed to the difference in the organization of hydrophilic segments during the nanoparticle formation. A higher hydrophilic/hydrophobic balance could reduce the interactions between the hydrophobic segments and generate large nanoparticles.

Table 1. Characterization of nanoparticles from **PA3** and **PA2,3** derivatives.

	Weight %[a]	D_h **(nm)**[b]	**PDI**[c]	**CMC (mg/L)** [d]
PA3-100	100	177	0.152	6.0
PA3-63	71	160	0.133	4.5
PA3-36	55	145	0.157	3.5
PA3-14	20	111	0.129	3.0
PA2,3-3	53	109	0.198	2.5

[a] Hydrophilic repeating unit weight percentage. [b]Obtained by DLS measurements. [c]Determined by fluorescence using pyrene as a probe.

Additionally, the study of **PA2,3-3** aqueous dispersion showed nanoparticles with a size of 109 nm (Table 1 and Figure 4a), lower than **PA3-36** which has a similar hydrophilic content. This fact shows the importance of the chemical structure of the hydrophilic and hydrophobic moieties in

the self-assembling process and the size of the nanoparticles. The analysis of aqueous polymeric solution by TEM showed the presence of well-defined spherical shape nanoparticles with different average diameters (Figure 4b). To determine the critical micelle concentration (CMC), as fundamental parameter of the micellation behavior of amphiphilic copolymers in aqueous dispersions, pyrene was used as a fluorescent probe. The intensity variation of fluorescence emission peaks at 384 and 374 nm confirmed the effective encapsulation of the hydrophobic probe and the self-assembling bringing the hydrophobic moieties into the cavities. CMC values between 3 and 6 mg/L were obtained, increasing as the hydrophilic content does for **PA3** derivatives, which is consistent with the general trend for amphiphilic copolymers (Table 1 and Figure S35).[27] Remarkably, a lower CMC value of 2.5 mg/L was determined for **PA2,3-3** (Figure 4c,d). These results demonstrate that the size of the copolymer micelles and therefore the behavior of micelles in aqueous solutions can be tailored by changing the modification degree, i.e, the hydrophilic/hydrophobic ratio. This parameter can be decisive in the rational design of tailor made nanoparticles for specific applications where the control of particle size and the stabilization of micelles play a crucial role as the case of *in vivo* drug delivery applications.

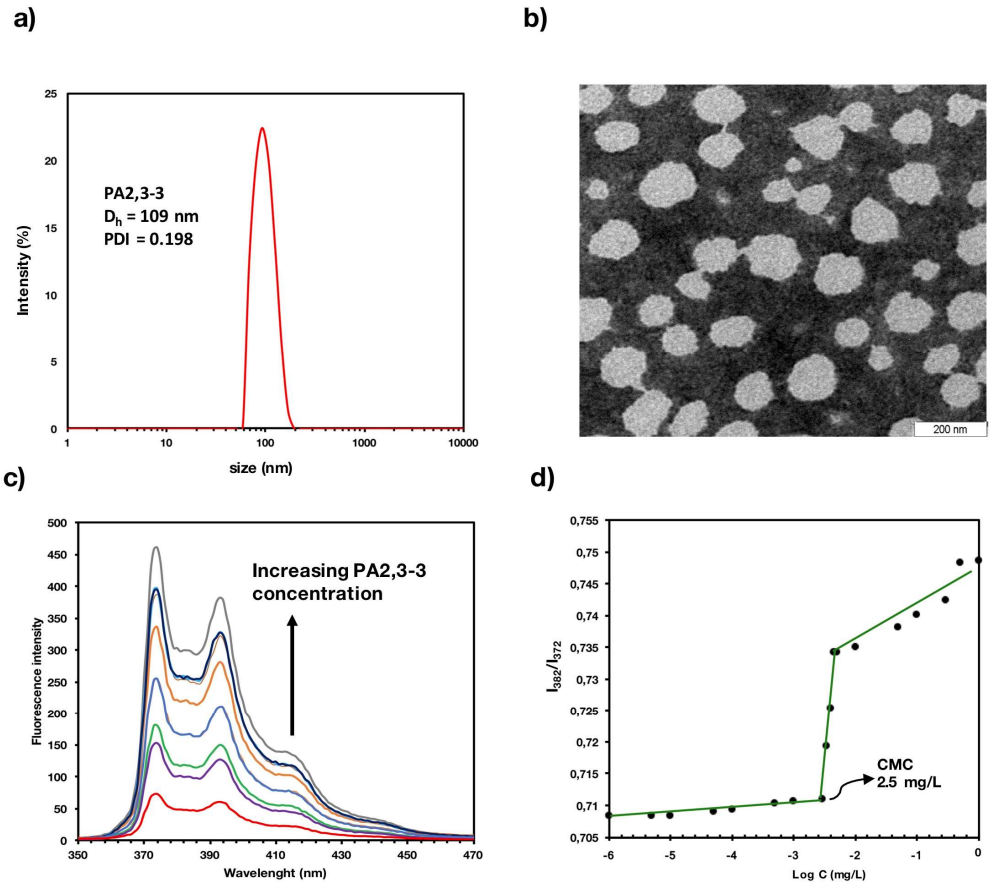

Figure 4. Characterization of **PA2,3-3** micelles: a) DLS size distribution for **PA2,3-3**, b) TEM image obtained after staining the micellar solution with phosphotungstic acid, c) Emission spectra of pyrene in **PA2,3-3** aqueous solution at different concentrations and d) Plot of the fluorescence intensity ratio (I_{382}/I_{372}) for pyrene vs the log of micelle concentration.

pH-Sensitivity of the amphiphilic polyacetal nanoassemblies: encapsulation and release of hydrophobic cargos

It is well-known that the hydrolysis of acetal moieties is rapid at low pH values and that they are relatively stable in neutral or alkaline media. **PA3-100** was selected as model polyacetal to further study the nanostructure disassembly of micelles at different acidity conditions (pH = 5.0 and 7.4).

The size change of nanoparticles was evaluated by DLS as shown in Figure 5. No significant size changes of **PA3-100** micelles were observed over 48 h at pH 7.4, which is in accordance with the stability of acetal groups in neutral media. However, when **PA3-100** micelles were subject to incubation at pH 5.0, an increase in the size of micelles can be clearly observed. For instance, the micelles expanded from 138 nm to about 350 nm in 6 h and reached about 450 nm and 600 nm in 12 and 24 h, respectively. Furthermore, the formation of 15 nm particles was detected after 72 h of incubation at pH 5.0, indicating the complete degradation of micelles in water-soluble monomers as a result of the complete acetal hydrolysis.

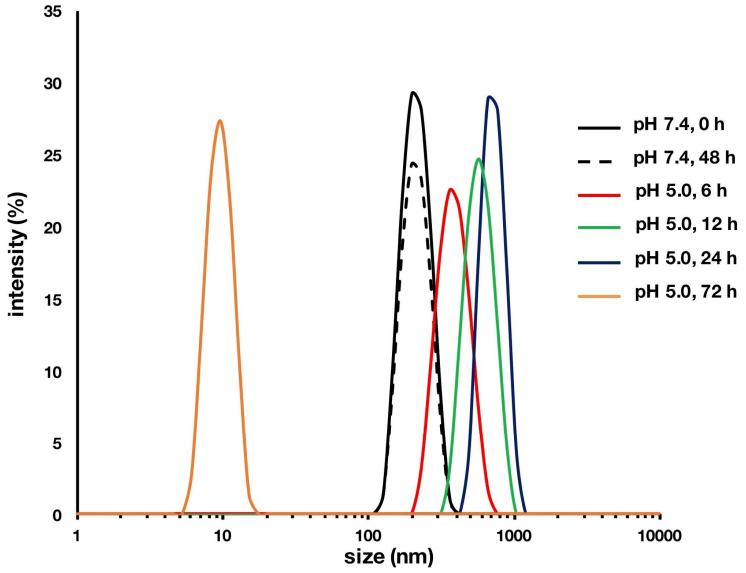

Figure 5. Time dependence of the size changes of **PA3-100** micelles during the exposure at pH= 7.4 and pH= 5.0.

These results encouraged us to investigate the potential of these amphiphilic polyacetals as a delivery system. Initially, we assessed whether the micelles could entrap a hydrophobic payload and made use of NR as a model compound. NR has been used extensively to study the self-assembly behavior of amphiphilic copolymers due to its poor solubility in water.[40] Their

absorption maxima strongly depend on the polarity of the surrounding environment. As general tendency, the λ_{max} of NR shifts from a higher value to a lower value with a decrease in the polarity of surrounding media. The encapsulation was accomplished by solvent diffusion from acetone into water. Quantification of the amount of encapsulated NR was done by UV-vis spectroscopy after filtration to remove non-encapsulated precipitated dye, freeze-drying and re-dissolving in THF. A clear shift in λ_{max} at 525 nm of NR encapsulated in micelles was observed when compared with the maximum absorption of NR in acetone, λ_{max} at 541 nm for **PA2,3-3**, suggesting the localization of NR inside the hydrophobic polyacetal core of the micelles (Figure S36). All the copolymers were able to encapsulate the hydrophobic probe to an extent of 78 to 90%. The encapsulation efficiency (EE) increases as the modification degree does, according to the increase of the particle size, being the copolymer **PA2,3-3** the polyacetal that display the best encapsulation value of 97% (Figure 6a).

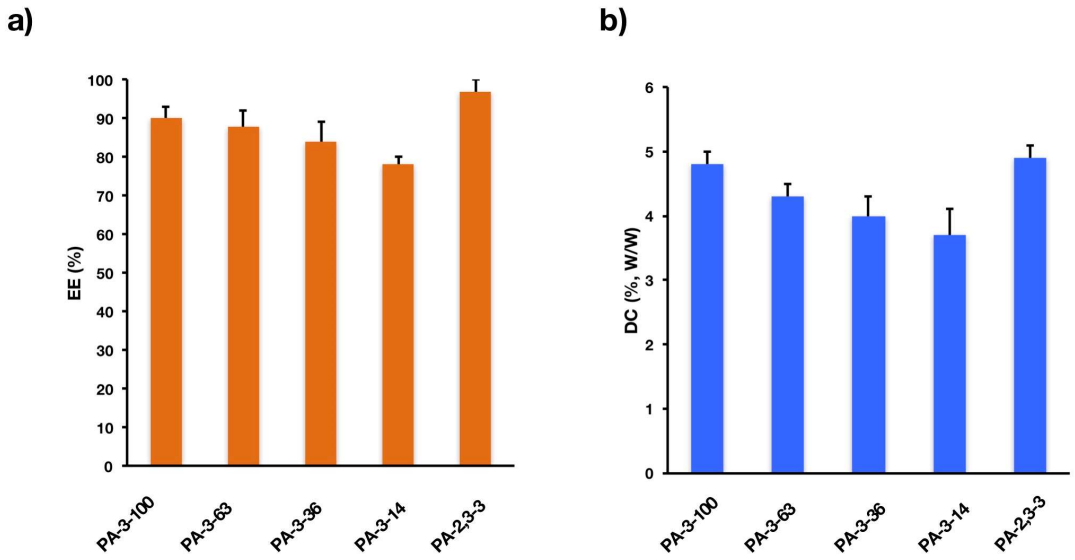

Figure 6. EE and DC value for amphiphilic polyacetals.

Next, to further study the potential of the functionalized polyacetals as nanocarriers, we focused on the loading and release of CUR, a prominent anticancer drug.[7] CUR-loaded micelles were prepared by solvent diffusion from acetone into water. To estimate the loading capacity, the lyophilized CUR-loaded micelles were redissolved in THF and analyzed by fluorescence spectrometry using a standard curve method. The drug loading content (DC) was determined to vary between 3.7 and 4.8%, at a theoretical drug loading of 5% (Figure 6b). The value of DC increases as the modification degree does, showing great drug encapsulation abilities for the tailored polyacetals. As in the case of EE determination, **PA2,3-3** showed the higher value (4.9%) for DC which make it the best candidate among the synthetized polymers for application as a delivery system.

We further analyzed the release behavior of CUR from micelles under both physiological conditions (pH= 7.4) and mild acid conditions (pH= 5.0) at 37 ºC using dialysis method (Figure 7). The results showed that the release of CUR from all the copolymers was faster at mild acidic pH than at physiological pH conditions. These obvious results were in harmony with the literature in which the disruption of acetal linkages takes place in acidic conditions while at neutral conditions they remain stable.[5] For instance, the cumulative percentage release demonstrated that the amount of CUR released from micelles was gradually increased over time and after 9 h, all the polyacetals showed more than 50% of CUR release at pH= 5 and less than 15% at pH= 7.4. The exposition to longer incubation times gives a maximum CUR release of 70% and 26% at pH= 5 and 7.4 respectively. Noticeably, the drug release slightly increases with the increasing the hydrophilic/hydrophobic balance for the **PA3** copolymers. Thus, 48%, 51%, 56% and 58% of CUR were released in 9 h at pH= 5.0 from **PA3-14**, **PA3-36**, **PA3-63** and **PA3-100**, respectively (Figure 7b,c,d,e). This fact can be attributed to the higher hydrophilic content that could force the

formation of looser micelles and then promote a slightly faster hydrolysis. In the case of **PA2,3-3** no significant differences in the degradation profile were observed in comparison with the **PA3-36** and **PA3-14**, containing the higher hydrophobic balance (Figure 7f).

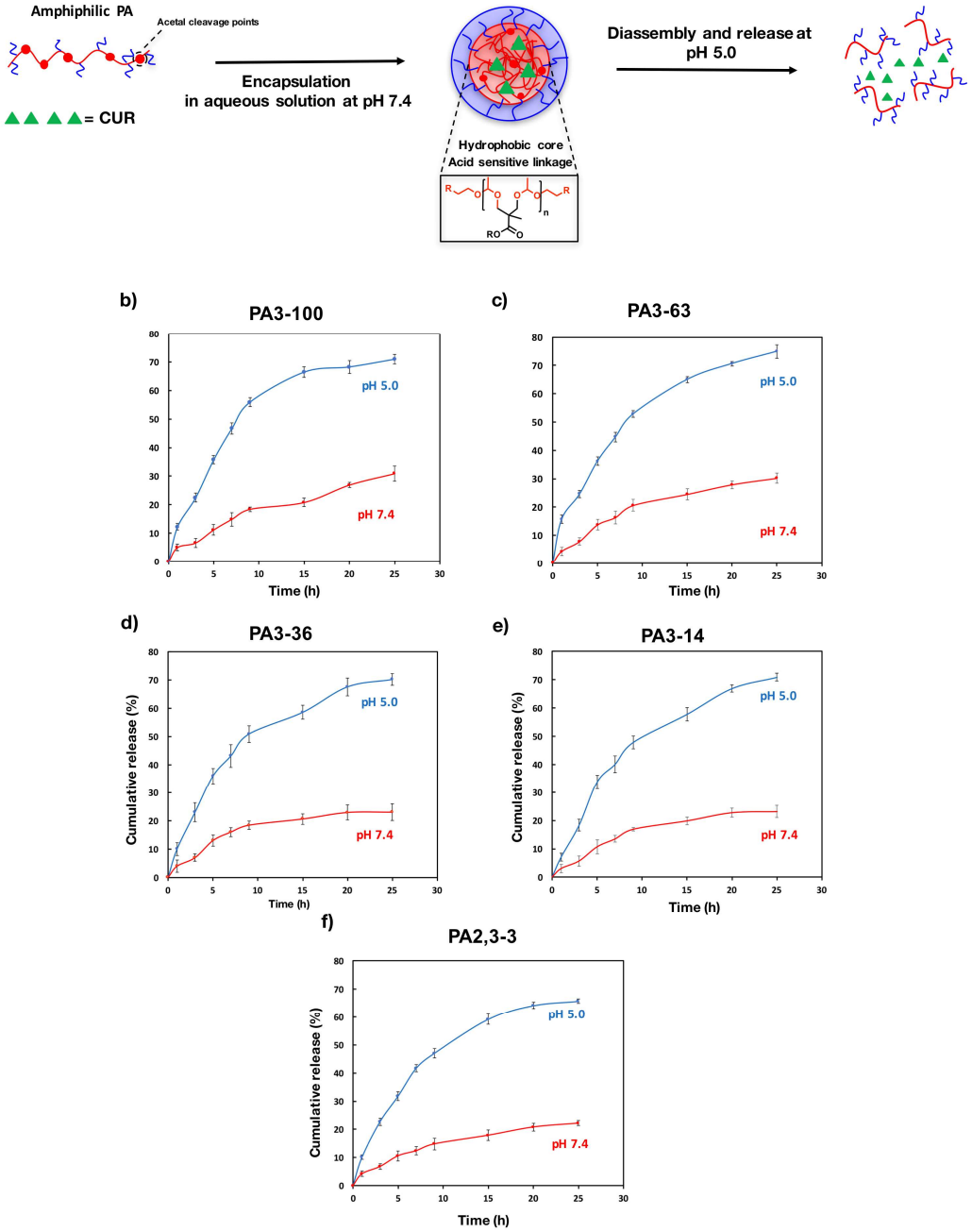

Figure 7. a) Schematic representation of encapsulation of CUR and release in mild acid conditions, b, c, d, e and f) release kinetics from **PA3-100**, **PA3-63**, **PA3-36**, **PA3-14** and **PA2,3-3** respectively.

As has been previously demonstrated, **PA-2,3** could be double functionalized via thiol-yne reaction and transesterification of the activated ester, showing its potential transformation *via* orthogonal chemistry. Moreover, the thiol-yne functionalization using ME lead a well-defined **PA-2,3-3** able to form micelles with high EE and DLC which degrade under mild acidic media, thus being suitable systems for drug delivery. Encouraged by these results and envisioning the high potential of this polyacetal, we planned to combine the functionalization of **PA2,3** with ME and the amidation of the hexafluoisopropyl moiety with a folate spacer (FS). In this way, a drug delivery system with the ability to deliver the drug content to specific sites by the selective interaction of the folate conjugate with specific cells as tumorous cells, could be obtained (Scheme 3).[38]

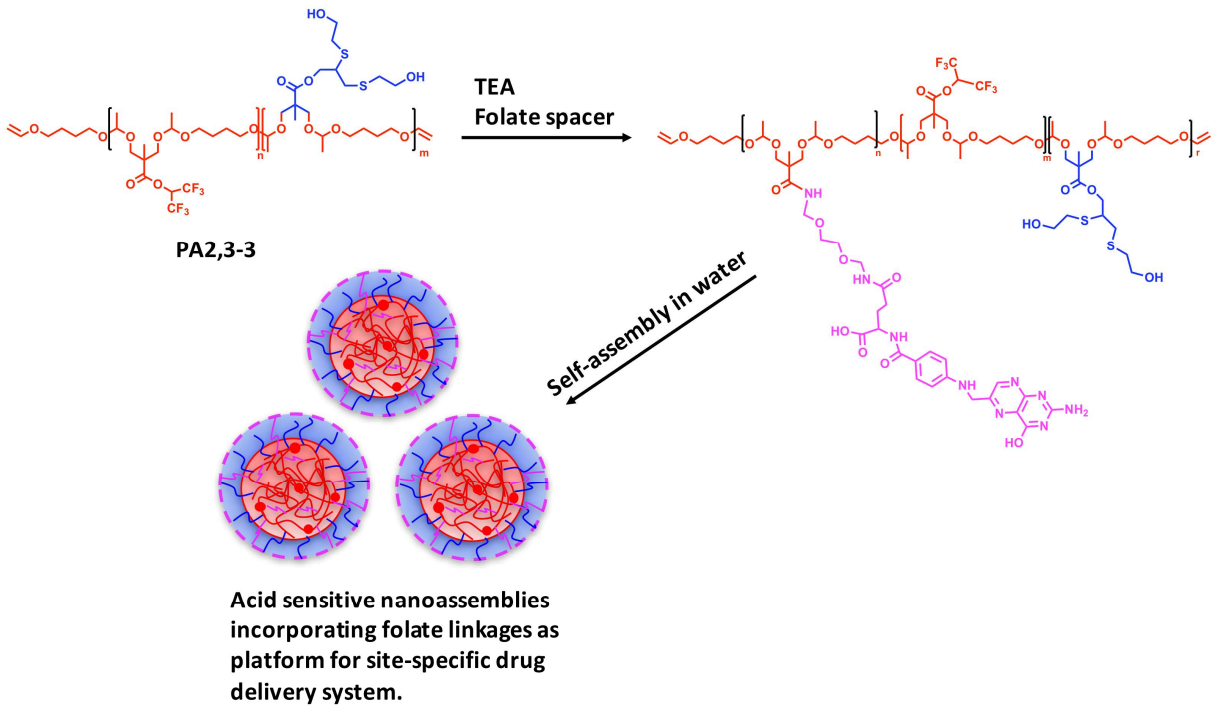

Scheme 3. Synthetic approach for the design of acid sensitive micelles decorated with folate groups based on amidation of amphiphilic **PA2,3-3** with FS.

Thus, **PA2,3-3** was subjected to amidation with the amino FS derivative to obtain **PA2,3-4** (SI-5 and SI-6). The reaction was monitored by ^{1}H NMR and ^{19}F NMR and after 24 hours the conversion of 100% was reached (Figure 8a). The ability of the copolymers to self-assembly in aqueous solutions was tested as has been above described. Delightfully, the analysis of aqueous dispersion of **PA2,3-4** by DLS revealed the formation of monodisperse assemblies with an average size of 167 nm (Figure 8b). The determination of CMC using pyrene as prove lead a value of 2.7 mg/L. Last but not least, the encapsulation and release of CUR as drug model was also evaluated. The release profile for **PA2,3-4** showed a similar trend than the polymer **PA2,3-3**, with a release of more than 50% of CUR the first 9 h and a maximum release of 70% after 15 h. (Figure 8c). These results demonstrate that after the modification of the activated ester moiety the obtained polyacetal was able to self-assembly to form micelles in water and keep showing good features for their use as site specific drug delivery system.

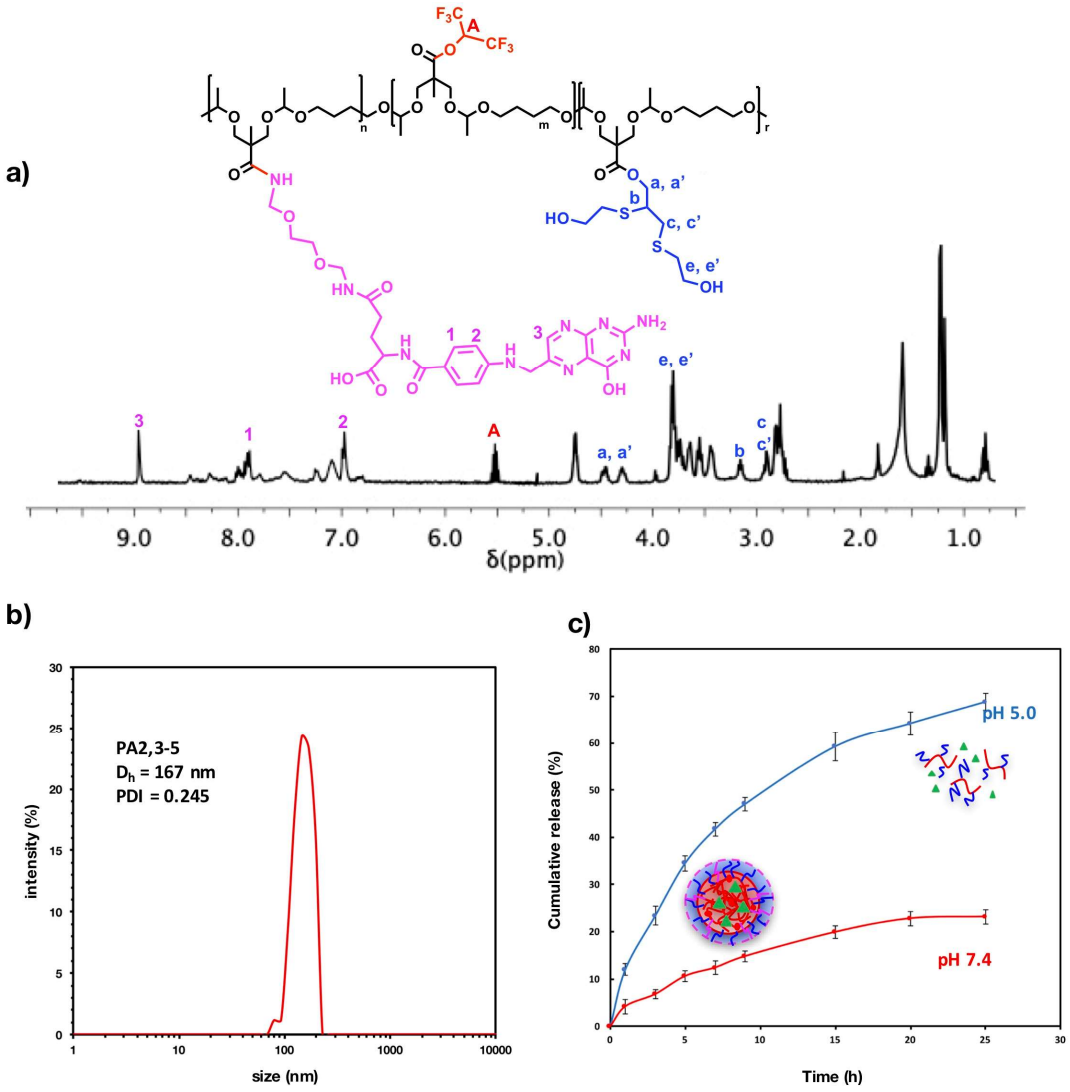

Figure 8. a) ^{1}H NMR spectra of **PA2,3-4**. b) DLS size distribution of **PA2,3-4** aqueous micellar solution and c) Release kinetics in neutral and mild acidic conditions for **PA2,3-4**.

Conclusions.

For the first time, the synthesis of highly tunable polyacetals was achieved *via* the polyaddition of functional diols (**M2** and **M3**) to DVE in mild reaction conditions. The double functionalization of **PA2,3** via thio-yne click reaction and subsequent transesterification of the activated ester shows the highly tunable character of these polymers through simple chemical transformations. The potential of this approach was demonstrated by the synthesis of amphiphilic polyacetals *via* the modification of **PA3** and **PA2,3** with ME. The obtained polymers were able to self-assembly in water and to form monodisperse nanoassemblies. Moreover, the possibility to target different degrees of functionalization was explored for **PA3** (100%, 64%, 34% and 14% respectively) and their direct effect in the particle size formation was observed, showing the possibility to tuning the CMC by the simple variation of modification degree. Micelles obtained in this way showed interesting features as drug delivery candidates (i.e., high EE and DC). Ultimately, **PA2,3-3** was decorated with a FS derivative *via* the amidation of activated ester and evaluated as a possible specific site drug delivery system. The results showed that after modification, the ability of the polyacetal to self-assembly in water, load CUR as a model drug and release it, is not altered. Therefore, this methodology represents a readily alternative to the rational design of site-specific drug delivery systems or more complex delivery systems based on the inclusion of target ligands to specific site action.

ASSOCIATED CONTENT

Supporting Information.

Synthesis and characterization data of diol monomers and model compounds. ^{1}H, ^{13}C, ^{19}F NMR spectra of monomers, model compounds, polyacetals and copolyacetals. Additional data for polymer modification and micelles characterization

ACKNOWLEDGMENT

Financial support from the MINECO (Ministerio de Economia y Competitividad) (MAT2014-53652-R, MAT2017-8266) is gratefully acknowledged. G.L. acknowledges the Serra Húnter Programme (Generalitat de Catalunya). A. M. was supported by an FPI grant (BES-2015-072662) from MINECO. I. Armero is gratefully acknowledged for preliminary experiments.

References

1 A.C. Albertson and M. Hakkarainen, *Science,* 2017, **358**, 872-873.

2 S. Binauld and M. H. Stenzel, *Chem. Comm.,* 2013, **49**, 2082-2102

3 V. Delplace and J. Nicolas, *Nat. Chem.,* 2015, **7**, 771-784

4 A. Hufendiek, S. Lingier and F. E. Du Prez, *Polym. Chem.,* 2019, **10**, 9-33

5 B. Liu and S. Thayumanavan, *J. Am. Chem. Soc*., 2017, **139**, 2306-2317.

6 Y. Wu, Y. Xiao, Y. Huang, Y. Xu, D. You, W. Lu and J. Yu, *Biomacromolecules,* 2019, **20**, 1167-1177.

7 G. Rodriguez Escalona, J. Sanchis and M. J. Vicent, *Macromol. Biosci.,* 2018, **18**, 1700302.

8 D. N. Amato, Douglas V. Amato, O. V. Mavrodi, W. B. Martin, S. N. Swilley, K. H. Parsons, D. V. Mavrodi and Derek L. Patton, *ACS Macro Letters,* 2017, **6**, 171-175.

9 X. Hu , T. Yang , R. Gu , Y. Cui , C. Yuan , H. Ge , W. Wu , W. Li and Y. Chen, *J. Mater. Chem. C*, 2014, **2**, 1836-1843.

10 S. Hou, D. M. Hoyle, C. J. Blackwell, K. Haernvall, V. Perz, G. M. Guebitz and E. Khosravi, *Green Chem.*, 2016, **18**, 5190-5199.

11 K. A. Miller, E. G. Morado, S. R. Samanta, B. A. Walker, A. Z. Nelson, S. Sen, D. T. Tran, D. J. Whitaker, R. H. Ewoldt, P. V. Braun and S. C. Zimmerman, *J. Am. Chem. Soc.,* 2019, **141**, 2838-2842.

12 H. Matsukizono and T. Endo, *J. Am. Chem. Soc.,* 2018, **140**, 884-887.

13 A. Moreno, G. Lligadas, J. C. Ronda, M. Galià and V. Cádiz, *Eur. Polym. J.,* 2018, **108**, 348-356.

14 A. G. Pemba, J. A. Flores and S. A. Miller, *Green. Chem*., 2013, **15**, 325-329.

15 Y. Huang, S. Thannneeru, Q. Zhang and J. He, J. *Polym. Sci. Part: A Polym. Chem.,* 2018, **56**, 1815-1824.

16 E. Themistou and C. S. Patrickios, *Macromolecules*, 2006, **39**, 73-80.

17 R. C. Li, R. M. Broyer and H. D. Maynard, *J. Polym. Sci: Part A: Polym. Chem.,* 2006, **44**, 5004-5013.

18 T. Debsharma, F.N. Behrenst, A. Laschewsky and H. Schalaad, *Angew. Chem. Int. Ed*., 2019, **58**, 6718-672.

19 H. Sardon, J. M. W. Chan, R. J. Ono, D. Mecerreyes and J. L. Hedrick, *Polym. Chem.,* 2014, **5**, 3547-3550.

20 L. Li, C. He, W. He and C. Wu, *Macromolecules*, 2011, **44**, 8195-8206.

21 A. Nimmagadda, X. Liu, P. Teng, M. Su, Y. Li, Q. Qiao, N. K. Khadka, X. Sun, J. Pan, H. Xu, Q. Li and J. Cai, *Biomacromolecules*, 2017, **18**, 87-95.

22 M. Tesch, J.A.M. Hepperle, H. Klaasen, M. Letzel and A. Studer, Angew. Chem. Int. Ed,. 2015, 54, 5054-5059.

23 S. R. Samanta, R. Cai and V. Percec, *Polym. Chem.,* 2015, **6**, 3259-3270.

24 C. E. Hoyle, A. B. Lowe and C. N. Bowman, *Chem. Soc. Rev.,* 2010, **39**, 1355-1387.

25 D. Huang, F. Yang, X. Wang, H. Shen, Y. You and D. Wu. *Polym. Chem.,* 2016, **7**, 6154-6158.

26 S. Samanta, C. C. De Silva, P. Leophairatana and J. K. Koberstein. *J. Mater. Chem. B*., 2018, **6**, 666-674.

27 J. Zhao, H. Wang, J. Liu, L. Deng, J. Liu, A. Dong and J. Zhang, *Biomacromolecules,* 2013, **14**, 3973-3984.

28 R. A. Shenoi, S. Abbina and J. N. Kizhakkedathu, *Biomacromolecules*, 2016, **17**, 3683-3693.

29 J. Li, X. Zhang, M. Zhao, L. Wu, K. Luo, Y. Pu and B. He, *Biomacromolecules,* 2018, **19,** 3140-3148.

30 D. Huang, Y. Wang, F. Yang, H. Shen, Z. Weng and D. Wu, *Polym. Chem.,* 2017, **8**, 6675-6687.

31 F. Huang, R. Cheng, F. Meng, C. Deng and Z. Zhong, *Biomacromolecules,* 2015, **16**, 2228-2236.

32 F. Li, C. Chen, X. Yang, X. He, Z. Zhao, J. Li, Y. Yu, X. Yang and J. Wang. *ACS Appl. Mater. Interfaces,* 2018, **10**, 21198-21205.

33 P. Wei, G. Gangapurwala, D. Pretzel, M. N. Leiske, L. Wang, S. Hoeppener, S. Schubert, J. C. Brendel and U.S. Schubert, *Biomacromolecules,* 2019, **20**, 130-140.

34 T. Plyduang, A. Armiñan, J. Movellan, R.M. England, R. Wiwattanapatapee and M. J.Vicent, *Macromol. Rapid Commun.,* 2018, **39**, 1800265.

35 S. Samanta, C. C. De Silva, P. Leophairatana and J.T. Koberstein. *J. Mater. Chem. B*, 2018, **6**, 666-674

36 B. T. Luk and L. Zhang, *ACS Appl. Mater. Interfaces,* 2014, **6**, 21859-21873.

37 M. A. van Dongen, C. A. Dougherty and M. M. Banaszak Holl, *Biomacromolecules,* 2014, **15**, 3215-3234.

38 M. Bartz, F. Canal, K. Koynov, R. Zentel and M. J. Vicent, *Biomacromolecules,* 2010, **11**, 2274-2282.

39 H. Li, M. Miteva, K. C. Kirkbridge, M. J. Cheng, C. E. Nelson, E. M. Simon, M. K. Gupta, C. L. Duvall and T. D. Giorgio, *Biomacromolecules,* 2015, **16**, 192-201.

40 D. S. W. Benoit, S. Srinivasan, A. D. Shubin and P. S. Stayon, *Biomacromolecules,* 2011, **12**, 2708-2714.

41 R. Zagami, V. Rapozzi, A. Piperno, A. Scala, C. Triolo, M. Trapani, L. E. Xodo, L. M. Scolaro and A. Mazzaglia, *Biomacromolecules,* 2019, **20**, 2530-2544.

42 H. Liu, S. Li, M. Zhang, W. Shao and Y. Zhao, *J. Polym. Sci. Part A: Polym. Chem.,* 2012, **50**, 4705-4716.

43 C. Mangold, C. Dingels, B. Obermeier, H. Frey and F. Wurm, *Macromolecules*, 2011, **44**, 6326-6344.

44 R. J. González-Paz, G. LLigadas, J. C. Ronda, M. Galià, V. Cádiz, *Polym. Chem.* 2012, **9**, 2471-2478.